Noninvasively recorded high-gamma signals improve synchrony of force feedback in a novel neurorehabilitation brain-machine interface for brain injury

Flint RD, Li YC, Wang PT, Vaidya M, Barry A, Ghassemi M, Tomic G, Brkic N, Ripley D, Liu CY, Kamper D, Do AH, Slutzky MW. ***J. Neural Eng.*** 2022;19;036024.

Abstract

Objective. Brain injury is the leading cause of long-term disability worldwide, often resulting in impaired hand function. Brain-machine interfaces (BMIs) offer a potential way to improve hand function. BMIs often target replacing lost function, but may also be employed in neurorehabilitation (nrBMI) by facilitating neural plasticity and functional recovery. Here, we report a novel nrBMI capable of acquiring high-γ (70-115 Hz) information through a unique post-TBI hemicraniectomy window model, and delivering sensory feedback that is synchronized with, and proportional to, intended grasp force. *Approach*. We developed the nrBMI to use electroencephalogram recorded over a hemicraniectomy (hEEG) in individuals with traumatic brain injury (TBI). The nrBMI empowered users to exert continuous, proportional control of applied force, and provided continuous force feedback. We report the results of an initial testing group of three human participants with TBI, along with a control group of three skull- and motor-intact volunteers. *Main results*. All participants controlled the nrBMI successfully, with high initial success rates (2 of 6 participants) or performance that improved over time (4 of 6 participants). We observed high-γ modulation with force intent in hEEG but not skull-intact EEG. Most significantly, we found that high-γ control significantly improved the timing synchronization between neural modulation onset and nrBMI output/haptic feedback (compared to low-frequency nrBMI control). *Significance*. These proof-of-concept results show that high-γ nrBMIs can be used by individuals with impaired ability to control force (without immediately resorting to invasive signals like ECoG). Of note, the nrBMI includes a parameter to change the fraction of control shared between decoded intent and volitional force, to adjust for recovery progress. The improved synchrony between neural modulations and force control for high-γ signals is potentially important for maximizing the ability of nrBMIs to induce plasticity in neural circuits. Inducing plasticity is critical to functional recovery after brain injury.

Introduction

Brain injury from trauma or stroke is a leading cause of long-term disability worldwide, constituting a major public health concern (Dewan et al. 2018, Virani et al. 2021). For the individual, loss of fine motor control following a brain injury can restrict one's ability to carry out activities of daily living (ADLs) independently. Many ADLs depend on the ability to precisely regulate grasp force; unfortunately, brain injuries can compromise one's ability to generate and hold grasp force. To treat this and other deficits arising from brain injury, there is growing interest in approaches that use some form of neuromodulation to induce activity-dependent plasticity, as a supplement to traditional physical therapy (Soekadar et al. 2015, Krucoff et al. 2016). In particular, such approaches could create a pathway for individuals to participate in neurorehabilitation even if they lack any residual movement. Brain-machine interfaces (BMIs) can translate motor intent to action through the direct interpretation of brain signals sampled from motor cortices (Slutzky and Flint 2017, Slutzky 2019). BMIs have largely been designed to replace lost function, for example through control over robotics (Hochberg et al. 2012, Collinger et al. 2013, Balasubramanian et al. 2017) or functional electrical stimulation (FES; Do et al. 2011, Ajiboye et al. 2017). However, BMIs can also be used to help induce plasticity and facilitate neurorehabilitation (Ramos-Murguialday et al. 2013, Bundy et al. 2017,

Biasiucci et al. 2018). Here, we introduce a novel neurorehabilitation BMI (nrBMI) that enables users to exert continuous, proportional control of thumb force while receiving haptic feedback that is tightly synchronized to the onset of motor intent. This nrBMI design allows control to be shared between decoded intent and voluntary (active) force, to maximize engagement and promote recovery. The current results provide noninvasive proof of concept in support of a future high-γ driven nrBMI that will be implemented with invasively acquired signals, such as subdural surface potentials (electrocorticography or ECoG).

There are multiple ways that nrBMI-based therapies could help improve function. Feedback from nrBMIs can be provided on attempted motor execution, even without detectable movement or force. This in itself provides a powerful motivator and enabler of learning, since learning and recovery generally benefit from sensory feedback (Vidoni et al. 2010, Abela et al. 2012). Also, nrBMIs potentially can enable targeting of plastic changes to specific brain areas. Perhaps most relevant, previous work has shown that functional gains after stroke are possible using nrBMI control of an exoskeleton (Ramos-Murguialday et al. 2013, Hortal et al. 2015, Bundy et al. 2017, Frolov et al. 2017) or FES (Biasiucci et al. 2018). See also Cervera et al. (2018) and Carvalho et al. (2019) for meta-analyses indicating an overall benefit for nrBMI training after stroke.

In spite of the evidence that nrBMI use can be beneficial, challenges remain before nrBMIs can be widely used in clinical settings. One challenge regards the timing of feedback. Rehabilitation of function through Hebbian-type neural plasticity ultimately depends upon synchrony between pre- and post-synaptic neurons (Caporale and Dan 2008), so it will be crucial to synchronize feedback to motor intent. However, to date nearly all nrBMIs have relied on electroencephalography (EEG) or MEG, using relatively low-frequency (<40 Hz) portions of the spectral domain. This can result in feedback delays on the order of 1 s (King et al. 2014). Such delayed feedback may be one reason why it remains unclear whether low-frequency signals can foster the plasticity required for long-term functional gains (Bai et al. 2020). By contrast, high-γ band (>70 Hz) power has greater temporal resolution than low-frequency signals (Crone et al. 2001, Wang et al. 2016), which should enable greater synchrony, and therefore induce more plasticity. In addition, high-γ has more movement-related information than μ–β band, as shown with intracortical recordings (Stark and Abeles 2007, Zhuang et al. 2010, Flint et al. 2012a, Flint et al. 2012b) as well as ECoG (Ball et al. 2009, Pistohl et al. 2012, Flint et al. 2014). Thus, we hypothesized that employing high-γ for nrBMI control would allow users to exert continuous, proportional control over motor execution, instead of relying on classification of discrete command signals. This could enable (for example) an nrBMI that continuously decodes graded finger joint kinematics or grip force in real time, instead of classifying a binary, "open/close" grasp command. In an nrBMI, proportional control during therapy could be important to successfully inducing neural plasticity, by aligning feedback with expectations, both in timing and intensity. It also might enable recovery of more fractionated movement than is possible with discrete, binary classification methods.

High-γ signals can be obtained with implanted electrodes, at intracortical, subdural, or epidural levels, but high-γ is severely attenuated by the skull in traditional EEG. Here, we present a novel nrBMI that uses high-γ power from hEEG to control haptic feedback to the thumb in an isometric grasp-like force task. The hEEG platform enables us to prototype an nrBMI using high-γ before using implanted electrodes. It has been previously shown that high-γ motor information can be acquired using EEG recorded in the presence of a hemicraniectomy (hEEG; Voytek et al. 2010, Vaidya et al. 2019, Li et al. 2020b). Hemicraniectomy procedures are typically performed with individuals following severe traumatic brain injury (TBI) to prevent

brain herniation. Our research participants included individuals with varying degrees of hand weakness following TBI. The ability to accurately regulate force is a generally underserved area in BMI research (although see Downey et al. 2018, Flint et al. 2020, Rastogi et al. 2020), and the importance of force to functional grasp means that filling this gap is an important step toward clinically useful BMIs.

In this study, individuals with TBI were able to successfully control the nrBMI while receiving haptic feedback that was time-locked to the onset of force intent. Feedback control was shared between active (or attempted) force and decoded intent. We term this nrBMI-shared control. Importantly, we found that the synchronization of sensory feedback to motor intent was significantly tighter when using high-γ based nrBMI-shared control, compared to μ–β based nrBMI-shared control. These results provide a first step towards developing nrBMIs that sample high-bandwidth neural signals with high temporal precision for targeted therapy in a clinical setting.

Methods

Our ultimate goal is to develop an nrBMI that facilitates the recovery of function by promoting neural plasticity and helping users re-acquire motor skills that were lost after brain injury. In this study, we developed, tested, and validated a novel nrBMI at [names of institutions withheld during review]. All experimental protocols were approved by the respective Institutional Review Boards.

Target clinical population

We worked with human participants in two groups: (1) individuals with no brain injury and unimpaired motor function, and (2) individuals who had undergone decompressive hemicraniectomy following severe TBI. The inclusion criteria for group (2) were: minimal hyperalgesia, allodynia or neglect in the hand/arm (at least some residual pressure-sensation function was needed in the thumb); ability to tolerate wearing an EEG cap for a 2-hour session; ability to understand and follow instructions; and ability to attend to a task for at least five minutes at a time. We emphasize that weakness in the hand was not an exclusion criterion; our post-TBI participants included an individual with a score of 0 on the Medical Research Council muscle strength scale (MRC; No 1976), defined as “no visible contraction” of the thumb. Here, we present validation data from 3 participants with TBI (2 female; ages approximately 25-65, designated T1 through T3) and 3 control participants (3 male; ages approximately 20-30, designated N1 through N3).

nrBMI novel neurorehab platform: overview

The brain signals we acquired were EEG or hEEG. We specifically focused on modulations in high-γ power that occur with isometric thumb force (or attempted force). We provided haptic feedback using linear actuators to apply pressure (isometric force normal to the participant’s thumbnail) that was controlled by the intended force. We used frequency decomposition (via short-time Fourier transform) to calculate high-γ power in real time and decoded intended force continuously. The nrBMI translated this intended force into a haptic feedback force, applied it to the thumb, and measured both total force and haptic feedback force continuously. A visual feedback display was available to the participants, showing both task goals and a visual representation of instantaneous total force applied. Intact-skull participants used μ and β power to control the nrBMI. We envision a use-case where an individual with reduced hand function

uses the nrBMI to gain assistance in generating force, while receiving sensory feedback synchronized with their intent. Over time, with improvements in hand function, the degree of nrBMI assistance could be reduced, to facilitate strength-building and a path towards independent function.

EEG/hEEG acquisition

We acquired EEG or hEEG signals using a 128-channel actiCAP (BrainVision, Inc) together with a 128-channel Neuroport Multineuron Acquisition Processor (Blackrock Microsystems, Inc.). The actiCAP system embeds EEG electrodes with active electronics in a stretchable fabric cap. To optimize the signal quality in our recordings, we measured electrode impedance in real time at the beginning of each recording session, while applying gel. We targeted an impedance level of <25 kΩ for each electrode in these sessions. After applying gel, we wrapped the cap in kerlix gauze. In hEEG recordings, we placed gauze sponges above the craniectomy (below the kerlix), to maintain electrode-skin contact. A rendering of the EEG cap fitted to a participant with a hemicraniectomy (Structure Sensor Pro, Occipital, Boulder, CO) is shown in figure 1(a). The EEG and hEEG signals were lowpass filtered (500 Hz) and sampled at 2000 Hz. For participants with TBI, we removed 2-3 electrodes from the peripheral channels of the head cap, using them to record EMG at the trapezius and masseter muscles in preparation for an EMG-removal procedure (see 'Offline analysis', below).

Haptic device

In the experimental protocol, participants applied (or attempted) force with the thumb's palmar surface to match a random force level target (details in 'Visual feedback during hand control', below). Accordingly, we designed and constructed the haptic feedback device (figure 1(b)) to perform three main functions: (1) sense force applied by the palmar surface of the thumb (F_{active}); (2) apply pressure to the dorsal surface of the thumb (i.e., the thumbnail), forming an "assisted" pinch; and (3) sense the external force applied to the thumbnail, called F_{haptic}. We used two independent load cells (1 degree of freedom FC20-10kg, Forsentek, Shenzen, China) built into custom fittings in the haptic device to sense F_{active} and F_{haptic}. We produced haptic force feedback using a linear actuator (pq12, Acutonix, Victoria, Canada; figure 1(b)) mounted alongside two linear rails (Thompson, Radford, VA). This assembly was capable of applying a maximum of approximately 50 N feedback force to the thumb (Barry et al. 2018). The entire housing of the haptic device could be rotated, to maintain a comfortable and consistent wrist and forearm angle (45° internal forearm rotation, 0° wrist flexion). We designed and built custom electronics to amplify and filter the load cell output, power the actuators, and electrically isolate the haptic device's power and input/output from the participant and data acquisition equipment. This was done for participant safety, and to prevent signal contamination from mains power.

System calibration - force

This section of Methods, and the following four sections are laid out in order of a typical experiment. For all participants, we began experimental sessions by calibrating both force sensors (F_{active} and F_{haptic}), as well as the ergonomic limits of the force that could be applied by the BMI (F_{BMI}) for feedback. The participant's thumb was fixed in place for the duration of the experiment, by means of an adhesive Velcro sticker. During F_{active} sensor calibration, the participant was instructed to apply (or attempt) a firm pressure on the load cell (maximum voluntary force, MVF), holding it for approximately 1 s and releasing. Then, F_{BMI} and F_{haptic}

were calibrated simultaneously. The linear actuator was advanced until the feedback applicator (the part of the device that applied force to participant's thumb) lightly but continuously contacted the thumbnail. From there, the haptic applicator was advanced in small increments until just before the participant reported discomfort. This established the lower and upper limits of displacement for the haptic feedback device during nrBMI-shared control (described in *Software architecture: nrBMI-shared control,* below).

Visual feedback during hand control

As in previous work, [reference withheld during review], we used a behavioral task inspired by random-target pursuit tasks used in studies of reach kinematics. Visual feedback was presented to the participants on a monitor placed just above their hand. During hand control mode, the haptic feedback device did not apply force (i.e., F_{BMI}=0 and F_{haptic} = 0 throughout). The participant's voluntary force level (F_{active}) controlled the color of a section of a monitor's screen (figure 1(c)). The screen area being controlled was superimposed on a static image of a human thumb to encourage gaze fixation: the color of the thumbnail changed with the amount of force applied. The color scale ranged from cyan (low force) to purple (high force; figure 1(c)). All aspects of visual feedback were controlled by a custom-designed Python application, including randomization of target level and the internal state machine governing progress through the trial. Each trial consisted of a target force presentation with a timeout of 5 s. If the applied force matched within 10% of the target force level, the participant was cued to hold that level for at least 500 ms (figure 1(c)). A Success trial required matching the force level to the target level throughout the hold period, which increased the participant's score and was paired with a video-game like reward sound and visual cue for motivation. Exiting the target force level prior to the end of the hold period necessitated re-acquisition of the target and holding for a new 500 ms period (i.e., transitory matches of the target force level were not Successes). Each Success (or Failure, due to timeout) was followed by a 4 s inter-trial interval marked by a white border, during which participants were instructed to relax. For T1 (who was unable to exert voluntary hand force), instead of random force level targets we issued instructions to attempt 3 levels of force: light, medium, and firm thumb pressure. In this case, the visual feedback was not used for hand control, and we instructed the participant to concentrate on force attempts. Hand control recordings were used for building decoders (see next section), and for offline analysis.

Decoder construction

We prepared to conduct nrBMI-shared control experiments by using a fast decoder building procedure to prepare a decoder from hand control recordings on the same day (usually requiring <5 minutes to calculate). For N1-N3, we built decoders from EEG electrodes in rows F to P (10-5 labeling system; Oostenveld and Praamstra 2001) on the contralateral side of the hand used in testing (side to test chosen randomly). For T1-T3, we built the decoders from hEEG electrodes in rows F through P that were also located over the hemicraniectomy. In both participant groups, we manually rejected electrodes with high-amplitude artifacts contaminating the EEG signal. We performed a common-average re-reference on the remaining set. We then used frequency decomposition, similar to Flint et al. (2013), to generate frequency-domain features from the preprocessed signals. Briefly, we performed short-time Fourier transforms, followed by log normalization to calculate the power in frequency bins from 0 to the Nyquist frequency (sampling rate 2 kHz). We subtracted the mean (over the entire recording) from each frequency bin, then averaged across the band(s) of interest. For N1-N3, we used both μ (7-12 Hz) and β

(15-35 Hz) bands. For T1-T3, we used a single high-γ (70-115 Hz) band. We used these spectral features, along with force generated during hand control, to train a Wiener cascade decoder, which consisted of a linear Wiener filter (with ridge regression) convolved with a static nonlinearity (Korenberg and Hunter 1986). We built multiple Wiener cascade decoders on the hand-control dataset using 10-fold cross-validation, saving the highest-performing decoder for use in nrBMI-shared control.

Visual feedback during nrBMI-shared control

During nrBMI-shared control, visual task presentation was the same as in hand control: randomly selected force targets were presented as colors in a spectrum (see figure 1(c)). Here, control over visual feedback was shared between the participant's voluntary force F_{active} (when able), and nrBMI-controlled force measured by F_{haptic} (figure 1(d)). Visual feedback in nrBMI-shared control was governed by the equation

$$F_{total} = MVF\left(\mathcal{E}F_{active} + (1-\mathcal{E})F_{haptic}\right) \quad (1)$$

where color was directly controlled by F_{total}, MVF (maximum voluntary force) was a scale factor accounting for the maximum force the participant could exert (as measured during calibration, see 'System calibration - force' above), and $\mathcal{E}$ was the degree-of-sharing parameter. At $\mathcal{E} = 1$, control over the force color was the same as in hand-control mode; at $\mathcal{E} = 0$, the force color was entirely governed by the nrBMI output (scaled decoded force intent, or F_{BMI} in figure 1(d), see also next section). The shared-control paradigm allowed the nrBMI to be tuned to the individual's level of recovery, with higher proportion of control allotted to nrBMI output ($\mathcal{E}$ closer to 0) for those with less ability to generate F_{active} on their own. Thus, with changing ability (e.g., improvement of strength over time), the sharing parameter could be increased to require a greater degree of hand control, and thus increase the physical challenge to build strength. In these experiments, $\mathcal{E}$ was initialized according to each participant's hand strength using the MRC scale (0=no visible contraction, 5=normal strength). We set $\mathcal{E}$ to 0.1 for an MRC score of 0; otherwise, we set $\mathcal{E}$=MRC/10, where MRC was the participant's muscle strength score. The study was not designed to systematically vary $\mathcal{E}$, in part due to the limited time available with each participant (see Results).

Software architecture: nrBMI-shared control

The nrBMI was designed to provide haptic feedback that could be controlled by some combination of active force and modulation of brain signals. During nrBMI-shared control, the decoder output (F_{intent} in figure 1(d)) was passed via UDP interface to a custom-built virtual instrument (LabVIEW, National Instruments). There it was scaled according to participant-specific calibration of ergonomic force limits (see above 'System Calibration – force') to generate the nrBMI output (F_{BMI}). F_{BMI} was then appropriate to drive the linear actuator directly. F_{active} and F_{haptic} were sensed by the haptic feedback device's built-in sensors, and those signals drove the visual feedback for the participant (see previous section) via UDP communication between BCI2000 and the custom Python visual-feedback application. Overall, the system updated at a rate of 20 Hz (i.e., a bin size of 50 ms).

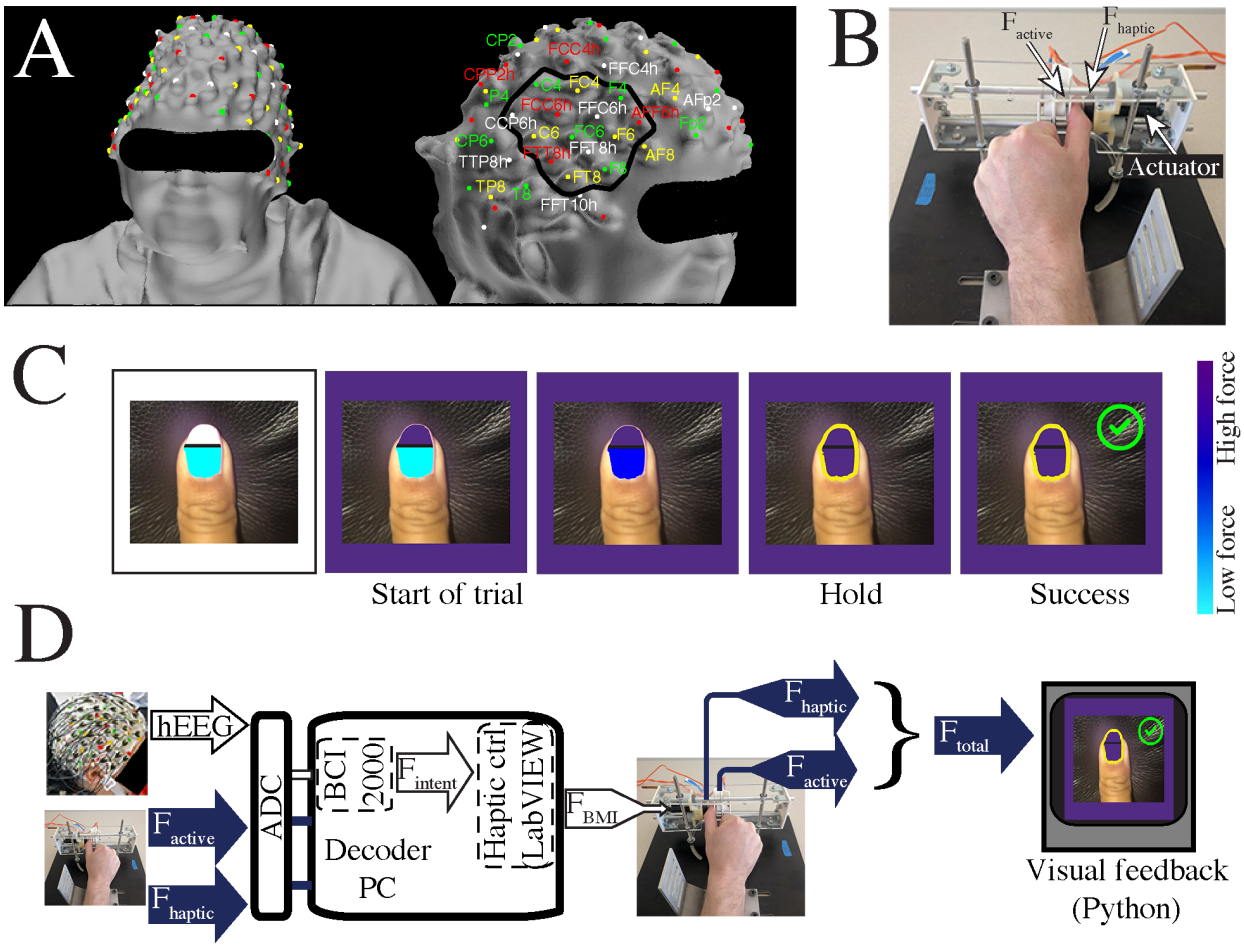

Figure 1. Overview of the neurorehabilitation BMI for force. (**A**) Participant T1 with electrode locations marked. The extent of the craniectomy is shown with a black outline. (**B**) The haptic feedback device. White arrows indicate sensor locations for F_{active} (force at palmar side of thumb, see main text) and F_{haptic} (external force applied to dorsal thumb surface), as well as the linear actuator. **(C)** Individual frames illustrating the progression of visual feedback during a trial. The target force is shown in the top half of the thumbnail image, while the current applied force (ranging from cyan to purple for low to high force, respectively) is shown in the base of the thumbnail. Target force (high force in this trial) is also shown around the outer border of the screen, except during rest periods, denoted by white (first image). Acquiring the target force level resulted in a yellow outline around the thumbnail. Successfully holding in the target for the hold duration produced a green success symbol. (**D**) System overview during nrBMI-shared control operation. Intended force was calculated by the nrBMI from brain signals, ultimately generating the haptic output F_{BMI}. F_{haptic} (generated by F_{BMI}) and F_{active} (generated by voluntary force) combined to generate F_{total} (main text, equation 1), which controlled visual feedback. During hand control, F_{haptic}=0 and visual feedback was controlled by F_{active} only.

Quantification of nrBMI-shared control performance

The success rate for nrBMI-shared control performance was the fraction of force targets that were successfully acquired. We also calculated a time-to-target (TTT) metric on Success trials, as the elapsed time between target presentation and the earliest time that the participant-controlled F_{total} matched within 10% of the target force. We note that for nrBMI-shared control, participant T1 (who lacked the ability to exert voluntary force) could be evaluated for performance using the same criteria as participants with healthy force-generating abilities. In addition to overall success rate, we also calculated success rate in a sliding window of 50 trials, allowing us to examine learning of the task over time.

Offline analysis: detecting modulation of high-γ in hEEG

To understand how high-γ modulation could drive BMI execution, we analyzed offline the signals recorded during BMI-shared control sessions. First, we cleaned the hEEG of electromyogram (EMG) artifact—a known complication when recording high-frequency EEG signals. We applied a technique called Electromyogram Removal by Adding Sources of EMG (Li et al. 2020a) to clean the hEEG. Briefly, this approach models EMG artifact in the hEEG signals by comparing it to real EMG (for example, collected from masseter or trapezius muscle) using independent components analysis. Independent components (ICs) identified as EMG are then subtracted, so the cleaned hEEG signal can be recovered from the remaining ICs. After cleaning hEEG using ERASE, we calculated the power amplitude as described above (see above, 'Decoder construction') and examined high-γ modulations in each electrode, averaged across trials in a window around force onset.

Validation: analysis of feedback lags for μ–β vs. high-γ control

We analyzed the delays between the onset of the participants' neural modulations and the onset of force generated by the nrBMI. We explored two relevant types of delays. First, we examined delays inherent to the nrBMI itself, i.e., the machine (computational and mechanical) elements of the brain-machine interface. Second, we quantified the lag associated with the type of neural signal (high-γ or μ–β) being used to control the nrBMI.

To establish a lower bound for inherent nrBMI delays, we tested the nrBMI step response. We performed two step response experiments; in each case using a simplified decoder that passed through a step input (5 V) with minimal processing, such that F_{BMI} was also a step. In the first experiment, we used a rigid block to transmit force applied by the haptic device (the F_{BMI} step output) directly to the F_{active} load cell. This simulated an idealized user-in-the-loop mode of nrBMI operation. In the second step response experiment, a volunteer's thumb was positioned in the haptic device and the step command from the nrBMI applied force to the thumbnail. The difference between the delays from the two step-response experiments revealed the amount of delay related to thumb compliance.

The second type of delay we examined was the lag in the detection of force intent from the hEEG (or EEG) features during nrBMI-shared control. Quantifying this lag allowed us to test our hypothesis that high-γ control results in greater temporal precision than μ–β control. To do this, we analyzed the data from participants who used high-γ features for nrBMI-shared control, compared to data from those who used μ–β features for nrBMI-shared control. Analysis of hEEG data began with cleaning via ERASE as in the previous section. Then, we found the onset of neural modulation in target electrodes (see next paragraph) and measured the lag between the neural modulation onset time and the time of F_{active} onset (figure 2).

To find the neural modulation onset time for an electrode, we first calculated the event-related feature perturbation (ERFP), which is found by averaging the overall event-related spectral perturbation (ERSP; Makeig 1993) across a frequency band of interest (high-γ or μ–β). ERSPs and ERFPs were calculated in a window of -1 to 0.1 s, aligned to F_{active} onset. From the ERFP, we calculated an index of modulation $IOM = F_R - F_B$, where F_B and F_R were the mean ERFP values in "background" and "response" segments, respectively. These were consecutive 0.25s sliding windows in the ERFP. We calculated IOM every 0.05 s. We inverted the sign of IOM for μ–β features, which decrease in power with motor onset. The neural modulation onset was taken to occur at the peak value of IOM, defining the lag due to nrBMI detection of force intent. See figure 2.

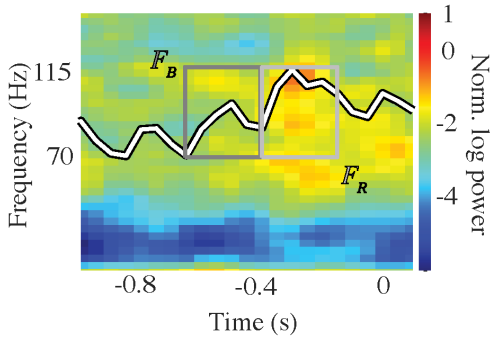

Figure 2. Calculation of feature modulation onset time for an electrode used in high-γ nrBMI-shared control. The ERSP, or trial-averaged spectrogram (colormap) was aligned to F_{active} onset (time 0). The high–γ ERFP (white-on-black line) was the trial-averaged mean spectral power in the 70-115 Hz frequency band. F_B and F_R were calculated from the dark grey and light grey boxes, respectively. Sliding these windows across the time course of the ERFP, we calculated $IOM = F_R - F_B$ at each time point (IOM curve not shown). The peak value of IOM was the onset time for the ERFP. In this example, the calculated onset of ERFP modulation was -0.4s.

Results

We recorded hEEG from three individuals who had undergone decompressive hemicraniectomies following TBI (participants T1,T2,T3). We also recorded standard EEG with three control (non-TBI) participants (N1,N2,N3), using μ–β signals for BMI execution.

Modulation of high-γ in hEEG

In designing the nrBMI, we targeted high-γ because of these signals' demonstrated capacity to carry detailed information about motor intent. We examined high-γ signals from nrBMI-shared control sessions, trial-averaged around F_{active} onset. Figure 3(a) shows high-γ power increase in two post-TBI participants, occurring just prior to force onset. We emphasize that it is ordinarily not possible to measure high-γ modulations in EEG signals, as exemplified in figure 3(b), which shows an ERSP from a non-TBI participant.

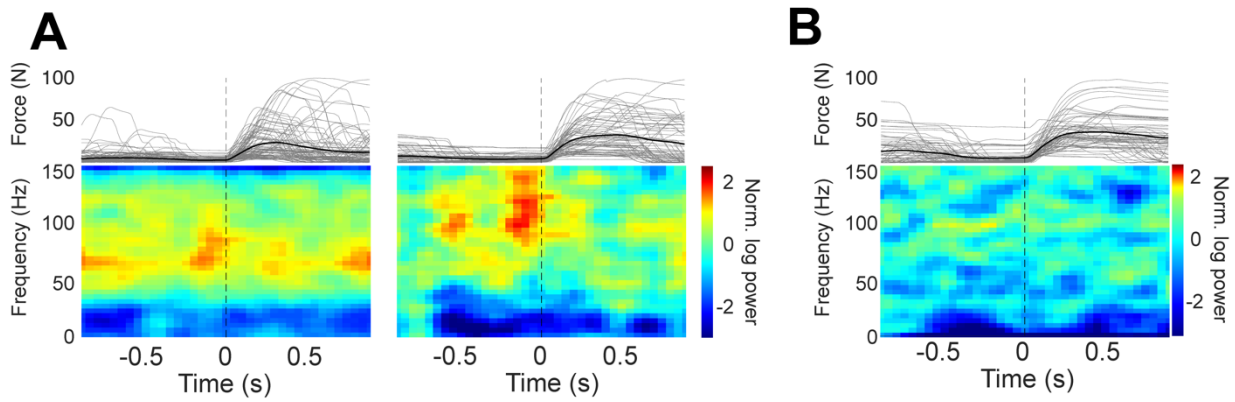

Figure 3. Example spectral variation relative to F_{active} onset during nrBMI-shared control. (**A**) Example ERSPs from T1 and T3, respectively (high-γ nrBMI-shared control). (**B**) Example ERSP from N3 (μ–β nrBMI-shared control). *Top*: single-trial force traces (gray) and trial averaged force (black) aligned to force onset (vertical dashed line). *Bottom*: mean spectrograms across trials.

nrBMI-shared control performance

Using high-γ hEEG (or μ–β EEG) modulations for nrBMI-shared control, all six of our participants were able to match force targets successfully (Table 1). Type of control (high-γ or μ–β) was not a significant source of difference in the mean time-to-target (TTT; t-test, p=0.81).

We note that participant T1, who scored 0 on the MRC strength scale (indicating no detectable active thumb flexion force), successfully used the nrBMI to exert some degree of force on a majority of trials, despite a relatively low overall success rate. We also found evidence of improved success over trials for 4 of 6 participants, including T1 (figure 4). Success rates for N1, N3, T2, and T3 all encountered a ceiling effect at 100% success and could not improve farther. Success rate for N1 and T2 began at approximately 100% and remained largely flat throughout their recording sessions.

The degree-of sharing parameter ($\mathcal{E}$ in equation 1) was initialized for each participant according to their muscle strength on the MRC scale (see Methods). Due to a limited number of recording sessions in most participants, we were not able to systematically test effects of varying $\mathcal{E}$; instead, we varied $\mathcal{E}$ empirically to maximize user engagement. There was no significant correlation between $\mathcal{E}$ and success rate in these data (R=-0.2, p=0.4, Pearson's coefficient).

Participant	Sessions; Runs	MRC strengt	EEG feat. used	Trials	Success Rate	TTT (s)	Norm. log power increase	Days since injury
N1	1; 1	5	μ–β	61	100%	1.8 ± 1.5	(1.9 ± 0.4)	N/A
N2	1; 4	5	μ–β	124	60%	2.3 ± 1.7	(2.2 ± 0.3)	N/A
N3	1; 5	5	μ–β	130	90%	1.7 ± 1.3	(2.3 ± 0.4)	N/A
T1	1; 5	0	high–γ	159	28%	2.3 ± 1.7	2.1 ± 0.25	92
T2	2; 2	5	high–γ	74	99%	2.8 ± 1.0	2.1 ± 0.2	79
T3	3; 11	5	high–γ	256	60%	1.2 ± 1.2	2.3 ± 0.5	52, 54, 57

Table 1. Summary of nrBMI-shared control performance across all trials. Sessions are equivalent to recording days; Runs are individual recording blocks (approximately five minutes duration). Time to target (TTT) and the increase or decrease in normalized log spectral power are reported as mean ± s.d.

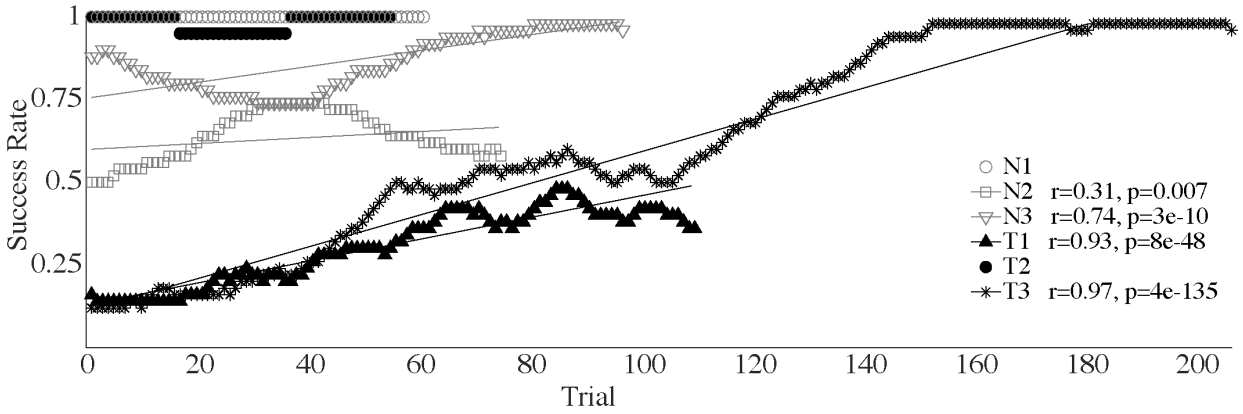

Figure 4. Success rate in a 50-trial sliding window. Solid lines show linear fit. Pearson's correlation coefficient for each subject is shown in the legend. N1 and T2 had no significant correlation between trial and success rate.

Temporal precision of haptic feedback in high-γ vs. μ–β control

One goal of providing somatosensory feedback during rehabilitation is to help trigger plasticity in neural circuitry, ideally promoting re-learning or adaptation as a means to restore function. Thus, the timing of feedback delivery should be a key factor in improving functional outcomes. With this in mind, we examined the delays between the onset of the participants' neural modulations and the onset of haptic feedback delivered by the nrBMI.

We did two step response experiments to quantify feedback delays (see Methods). The results of these step response experiments are shown in figure 5(a). In the first experiment, we used a rigid block to transmit force applied by the haptic device directly to the load cell (figure 5(a), left). In the second step response experiment, a volunteer's thumb was placed in the haptic device and passively allowed the step output from the nrBMI to apply force to their thumbnail (figure 5(a), right). Across both step response experiments, the time between the step input and F_{BMI} onset averaged 0.031 ± 0.003 s. Overall, the time between the step input and F_{active} onset in the rigid-block experiment was 0.104 ± 0.013 s (figure 5(a), inset), implying that approximately 0.07 s delay could be attributed to sources like communication between BCI2000 and LabVIEW, or time for the linear actuator to overcome inertia. When a human thumb was used in the nrBMI, the time between step input and F_{active} onset was 0.23 ± 0.014 s (figure 5(a), inset). Therefore, approximately 0.13 s of the overall delay can be attributed to the compliance of the thumb.

Next, we tested the hypothesis that high-γ confers an advantage (in feedback timing precision) over μ–β when it comes to driving the nrBMI. Using data from nrBMI-shared control in our participants, we calculated trial-averaged features (high-γ or μ–β) around F_{active} onset, and identified the neural modulation onset time for each electrode (see Methods, figure 2). Figure 5(b) shows the results, including only electrodes in the C row to focus specifically on the motor cortex signal. Across participants, on average F_{active} lagged neural modulation onset time by 0.38 ± 0.09 s for high-γ control (figure 5(b), red), while F_{active} onset lagged μ–β modulation by 0.61 ± 0.06 s (figure 5(b), blue). Thus, high-γ nrBMI users received haptic feedback significantly faster than μ–β nrBMI users (2-tailed t-test; $p = 0.008$). Neglecting physical delays arising from nrBMI processing and thumb compliance, the nrBMI detected a change in high-γ power approximately 150 ms after the actual start of neural modulation. This was more than twice as fast as when the nrBMI operated in the μ–β range, where approximately 380 ms was required to detect the onset of neural modulation. This finding has implications for neurorehabilitative

BMIs generally, as quicker feedback is more likely to trigger plasticity and enhance learning.

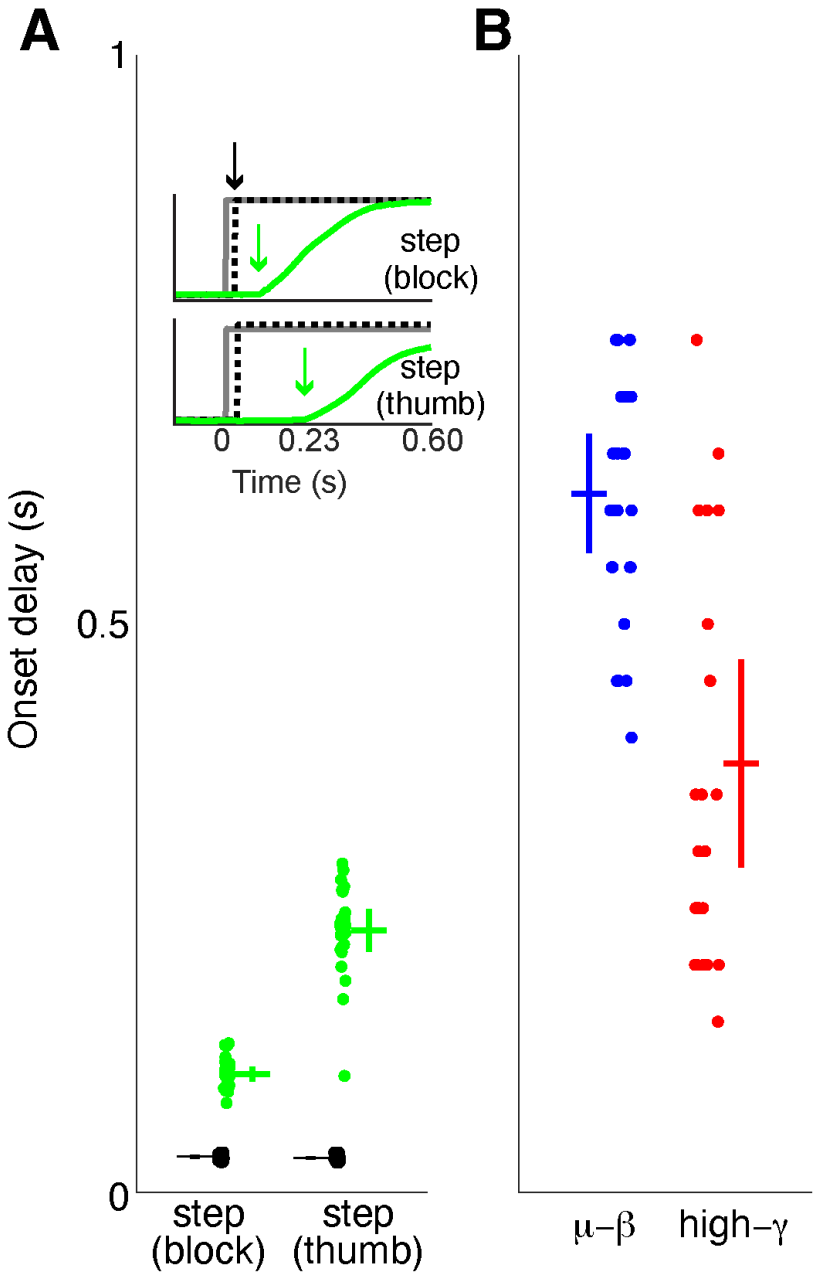

Figure 5. Timing of nrBMI haptic feedback. **(A)** Delays between step input and F_{BMI} (black) or F_{active} (green) onset. Inset plots show example trials from both step response tests. In both tests, step inputs (inset; solid grey lines) passed through simplified BMI decoders, generating F_{BMI} (inset; black dashed line). Black circular markers show the F_{BMI} delay (also shown in the inset with a black arrow); black horizontal lines show the mean F_{BMI} delay across trials; black vertical lines show the (very small) F_{BMI} delay s.d. Green circular markers and horizontal/vertical makers show the delay between step input and F_{active} onset, in a similar manner. Green arrows (inset) show example single-trial F_{active} onset delay. **(B)** similar to (A), but showing delays between neural modulation onset and F_{active} onset for μ–β (blue) or high-γ (red) nrBMI-shared control.

Discussion

Functional recovery after neurological trauma relies on plasticity within the nervous system. This plasticity has finite natural limits, as evidenced by the high number of individuals who experience chronic impairments following brain injuries like TBI (Schneider et al. 2021) and stroke (Furie 2020). In cases where biological plasticity is insufficient to promote motor recovery, it may be possible to use nrBMIs to augment this process. EEG-based nrBMIs have shown some success in improving movement function (Ramos-Murguialday et al. 2013, Bundy et al. 2017, Biasiucci et al. 2018). In this study, we demonstrated a nrBMI that included several novel elements. We successfully implemented a closed-loop nrBMI that decoded continuous, proportional grasp force intent from high-γ signals. The nrBMI also used a novel form of nrBMI-shared control between the decoded force intent and residual hand force. Participants learned to control the nrBMI with high success, especially when given the opportunity to practice. More importantly, we found that high-γ activity provided greater temporal precision in controlling the BMI than did low-frequency bands typically used in nrBMIs.

The haptic feedback provided by the nrBMI simulated the somatosensory experience of successful hand force, providing a potential means to facilitate plasticity and learning in the motor-sensory system. Both TBI and non-TBI participants were able to control the BMI, experience force feedback, and use the applied force to match a series of random force targets. In fact, we found no significant differences in the success rates or TTT between the two participant groups. This is encouraging in terms of the potential for brain-injured patients to use the nrBMI. There was evidence that the participants improved their nrBMI-shared control success rate over time, even when significant hand weakness was present. The amount of time spent with the participants was often limited (due to factors discussed below), which in some cases might have constrained their ability to achieve higher overall success rates. Moreover, we note that—while not directly measured in this report—the ultimate purpose of an nrBMI is to generate plasticity, rather than to achieve a high success rate.

We believe that the use of shared control, i.e., using the nrBMI to augment the residual grasp force, could be an important design element in nrBMIs. Most existing nrBMIs use the brain signal alone to control some version of haptic feedback or functional electrical stimulation (for a recent review, see Mansour et al. 2022). In contrast, our design enables scaling the assist level to the participant's level of impairment. This, in turn, encourages the user to produce as much active force as they are able in each trial, which may help retrain new or enhanced connections spurred by the nrBMI. Further, shared control may help maintain user focus and engagement, as it maximizes existing sensory feedback. The shared control approach used here could also be used in nrBMIs providing different types of feedback, such as exoskeletons. The current dataset did not reveal a significant correlation between the degree-of-sharing and nrBMI success rate.

We found a significant advantage to using high-γ for the nrBMI, as the feedback experience for T1-T3 (measured by F_{active} onset) was more tightly time-locked to their neural modulation onset than μ–β signals used by N1-N3. In fact, high-γ control delivered feedback approximately twice as quickly as μ–β, after accounting for physical delays (software and mechanical) in the nrBMI. The nrBMI described here had substantial inherent delays, possibly due to not being optimally designed for speed. With optimization, feedback could occur within as little as 150 ms given high-γ control, or potentially even sooner if bin sizes were shortened or updated more frequently. It remains to be determined whether there are specific temporal bounds for the induction of plasticity through nrBMI use. Plasticity in cortical neurons with single-unit BMI

control has been demonstrated (Ganguly et al. 2011), as has the importance of feedback timing for enhancing functional improvements post-stroke (Mrachacz-Kersting et al. 2016). Intuitively, more precise synchronization between motor intent and sensory feedback implies a higher potential to trigger Hebbian-type neural plasticity, which is one of the primary goals of neurorehabilitation therapy (Soekadar et al. 2015). While the use of a high-γ nrBMI to drive plasticity is a novel approach, high-γ modulation has been linked to cortical plasticity in general (Traub et al. 1998, Headley and Weinberger 2011) and M1 plasticity in particular (Nowak et al. 2017). Perhaps most relevant, the enhancement of high-γ modulations (via stimulation) has been shown to restore plasticity to impaired motor cortex (Guerra et al. 2020). With the potential for coincident activation (timing overlap between motor intent and haptic feedback), it seems likely that high-γ control could enable nrBMIs to generate greater plasticity, and hence more functional improvement, after brain injuries.

The current study has some limitations, chief among which is the relatively small sample size of participants. Data collection in the hospital setting was challenged by the Covid-19 pandemic, which severely limited (and periodically eliminated) access to research participants. We chose to publish these results as proof of concept, or early evidence that continuous, proportional nrBMI control of isometric force could be achieved using hEEG signals, and that using high-γ for nrBMI control is beneficial in terms of feedback synchrony. The nrBMI performance, or success rate (Figure 4) is not a functional outcome; we do not report functional outcomes in this proof-of-concept report. Instead, successful nrBMI control, combined with very short feedback delays, indicates that an individual could use the nrBMI to receive sensory feedback that is tightly locked to their motor intent, even while lacking the ability to generate volitional force. This makes the nrBMI a potentially valuable tool for inducing plasticity in the motor-sensory system. Future studies should quantify participants' degree of functional improvement, as measured by standard clinical outcomes.

Working with participants who had hemicraniectomy following TBI made it possible to access high-γ neural signals; however, there are some drawbacks that can accompany the post-TBI clinical profile. Although the scalp was unbroken in our participants, sensitivity of the skin around the edges of the hemicraniectomy was common, and care was required when donning/doffing the electrode cap. During the study, we encountered individuals with substantial cognitive deficits (including attention and memory), allodynia in the affected hand, and headaches unrelated to the experimental procedures. In addition, it was important to guard against participant fatigue, as research sessions were completed largely during inpatient hospital stays, while maintaining full daily schedules of therapy. We anticipate that a translation to clinical use will require a version of the nrBMI that can be used by the individual alone, or with minimal help from therapists or caregivers. Ultimately, epidural or subdural recordings are probably a better way to provide high-γ signals for precisely targeting damaged brain areas with nrBMI therapy. Such signals provide a high amount of motor intent information (Flint et al. 2017, 2020) and stability for BMI use (Pels et al. 2019, Larzabal et al. 2021, Silversmith et al. 2021). Using epidural or subdural signals for nrBMI device design could help optimize tradeoffs in signal stability, invasiveness, device longevity, and richness of motor information (Slutzky and Flint 2017). At the moment, devices using these signals are still under investigation, but continue to improve in design and are advancing in clinical trials (Degenhart et al. 2018, Leinders et al. 2020, Moses et al. 2021). The results of this study, especially the increased temporal precision and movement-related information, indicate that high-γ based nrBMIs warrant further investigation for restoring movement to brain-injured patients.

Conclusion

We presented an nrBMI design that has the potential to improve therapy options for individuals with brain injury, especially those who lack residual motor function. An important feature of the nrBMI is the degree-of-sharing parameter, which can allow the clinician (or the individual) to determine the amount of assistance that is desired from decoded brain signal, in contrast with the amount of voluntary active force that must be provided by the hand. This feature can be adjusted to account for progress in recovery. Using high-γ signals for nrBMI control significantly improved the synchrony of haptic feedback, allowing participants T1-T3 to experience sensory feedback that was more closely aligned in time with the motor intent output signal. This improved synchrony is important for maximizing the ability of the nrBMI to induce plasticity in neural circuits, which is key to improved outcomes.

Acknowledgements

The authors wish to thank our research participants, and the clinical staff at our partner hospitals. Information regarding funding sources is being withheld during the peer review process. We declare that no conflicts of interest exist.

References

Abela, E., Missimer, J., Wiest, R., Federspiel, A., Hess, C., Sturzenegger, M. and Weder, B. (2012). "Lesions to primary sensory and posterior parietal cortices impair recovery from hand paresis after stroke." PLoS One **7**(2): e31275.PMC3282712

Ajiboye, A. B., Willett, F. R., Young, D. R., Memberg, W. D., Murphy, B. A., Miller, J. P., Walter, B. L., Sweet, J. A., Hoyen, H. A., Keith, M. W., Peckham, P. H., Simeral, J. D., Donoghue, J. P., Hochberg, L. R. and Kirsch, R. F. (2017). "Restoration of reaching and grasping movements through brain-controlled muscle stimulation in a person with tetraplegia: a proof-of-concept demonstration." Lancet **389**(10081): 1821-1830.PMC5516547

Bai, Z., Fong, K. N. K., Zhang, J. J., Chan, J. and Ting, K. H. (2020). "Immediate and long-term effects of BCI-based rehabilitation of the upper extremity after stroke: a systematic review and meta-analysis." J Neuroeng Rehabil **17**(1): 57.PMC7183617

Balasubramanian, K., Vaidya, M., Southerland, J., Badreldin, I., Eleryan, A., Takahashi, K., Qian, K., Slutzky, M. W., Fagg, A. H., Oweiss, K. and Hatsopoulos, N. G. (2017). "Changes in cortical network connectivity with long-term brain-machine interface exposure after chronic amputation." Nat Commun **8**(1): 1796.PMC5703974

Ball, T., Schulze-Bonhage, A., Aertsen, A. and Mehring, C. (2009). "Differential representation of arm movement direction in relation to cortical anatomy and function." J Neural Eng **6**(1): 016006

Barry, A., Ghassemi, M., Vaidya, M., Zheng, S., Wang, P., Do, A., Kamper, D. and Slutzky, M. (2018). Design of a Haptic Force Feedback System for Pinch. 40th Annual International Conference of the IEEE Engineering in Medicine and Biology Society, Honolulu, HI.

Biasiucci, A., Leeb, R., Iturrate, I., Perdikis, S., Al-Khodairy, A., Corbet, T., Schnider, A., Schmidlin, T., Zhang, H., Bassolino, M., Viceic, D., Vuadens, P., Guggisberg, A. G. and Millan, J. D. R. (2018). "Brain-actuated functional electrical stimulation elicits lasting arm motor recovery after stroke." Nat Commun **9**(1): 2421.PMC6010454

Bundy, D. T., Souders, L., Baranyai, K., Leonard, L., Schalk, G., Coker, R., Moran, D. W., Huskey, T. and Leuthardt, E. C. (2017). "Contralesional Brain-Computer Interface Control of a Powered Exoskeleton for Motor Recovery in Chronic Stroke Survivors." Stroke **48**(7): 1908-1915.PMC5482564

Caporale, N. and Dan, Y. (2008). "Spike timing-dependent plasticity: a Hebbian learning rule." Annu Rev Neurosci **31**: 25-46

Carvalho, R., Dias, N. and Cerqueira, J. J. (2019). "Brain-machine interface of upper limb recovery in stroke patients rehabilitation: A systematic review." Physiother Res Int **24**(2): e1764

Cervera, M. A., Soekadar, S. R., Ushiba, J., Millan, J. D. R., Liu, M., Birbaumer, N. and Garipelli, G. (2018). "Brain-computer interfaces for post-stroke motor rehabilitation: a meta-analysis." Ann Clin Transl Neurol **5**(5): 651-663.PMC5945970

Collinger, J. L., Wodlinger, B., Downey, J. E., Wang, W., Tyler-Kabara, E. C., Weber, D. J., McMorland, A. J., Velliste, M., Boninger, M. L. and Schwartz, A. B. (2013). "High-performance neuroprosthetic control by an individual with tetraplegia." Lancet **381**(9866): 557-564

Crone, N. E., Boatman, D., Gordon, B. and Hao, L. (2001). "Induced electrocorticographic gamma activity during auditory perception. Brazier Award-winning article, 2001." Clin Neurophysiol **112**(4): 565-582

Degenhart, A. D., Hiremath, S. V., Yang, Y., Foldes, S., Collinger, J. L., Boninger, M., Tyler-Kabara, E. C. and Wang, W. (2018). "Remapping cortical modulation for electrocorticographic brain-computer interfaces: a somatotopy-based approach in individuals with upper-limb paralysis." J Neural Eng **15**(2): 026021.PMC5841472

Dewan, M. C., Rattani, A., Gupta, S., Baticulon, R. E., Hung, Y. C., Punchak, M., Agrawal, A., Adeleye, A. O., Shrime, M. G., Rubiano, A. M., Rosenfeld, J. V. and Park, K. B. (2018). "Estimating the global incidence of traumatic brain injury." J Neurosurg: 1-18

Do, A. H., Wang, P. T., King, C. E., Abiri, A. and Nenadic, Z. (2011). "Brain-computer interface controlled functional electrical stimulation system for ankle movement." J Neuroeng Rehabil **8**: 49.PMC3247850

Downey, J. E., Weiss, J. M., Flesher, S. N., Thumser, Z. C., Marasco, P. D., Boninger, M. L., Gaunt, R. A. and Collinger, J. L. (2018). "Implicit Grasp Force Representation in Human Motor Cortical Recordings." Front Neurosci **12**: 801.PMC6220062

Flint, R. D., Ethier, C., Oby, E. R., Miller, L. E. and Slutzky, M. W. (2012a). "Local field potentials allow accurate decoding of muscle activity." J Neurophysiol **108**(1): 18-24

Flint, R. D., Lindberg, E. W., Jordan, L. R., Miller, L. E. and Slutzky, M. W. (2012b). "Accurate decoding of reaching movements from field potentials in the absence of spikes." J Neural Eng **9**(4): 046006

Flint, R. D., Rosenow, J. M., Tate, M. C. and Slutzky, M. W. (2017). "Continuous decoding of human grasp kinematics using epidural and subdural signals." J Neural Eng **14**(1): 016005.PMC5528155

Flint, R. D., Tate, M. C., Li, K., Templer, J. W., Rosenow, J. M., Pandarinath, C. and Slutzky, M. W. (2020). "The Representation of Finger Movement and Force in Human Motor and Premotor Cortices." eNeuro **7**(4).PMC7438059

Flint, R. D., Wang, P. T., Wright, Z. A., King, C. E., Krucoff, M. O., Schuele, S. U., Rosenow, J. M., Hsu, F. P., Liu, C. Y., Lin, J. J., Sazgar, M., Millett, D. E., Shaw, S. J., Nenadic, Z., Do, A. H. and Slutzky, M. W. (2014). "Extracting kinetic information from human motor cortical signals." Neuroimage **101**: 695-703

Flint, R. D., Wright, Z. A., Scheid, M. R. and Slutzky, M. W. (2013). "Long term, stable brain machine interface performance using local field potentials and multiunit spikes." J Neural Eng **10**(5): 056005

Frolov, A. A., Mokienko, O., Lyukmanov, R., Biryukova, E., Kotov, S., Turbina, L., Nadareyshvily, G. and Bushkova, Y. (2017). "Post-stroke Rehabilitation Training with a Motor-Imagery-Based Brain-Computer Interface (BCI)-Controlled Hand Exoskeleton: A Randomized Controlled Multicenter Trial." Front Neurosci **11**: 400.PMC5517482

Furie, K. (2020). "Epidemiology and Primary Prevention of Stroke." Continuum (Minneap Minn) **26**(2): 260-267

Ganguly, K., Dimitrov, D. F., Wallis, J. D. and Carmena, J. M. (2011). "Reversible large-scale modification of cortical networks during neuroprosthetic control." Nat Neurosci **14**(5): 662-667

Guerra, A., Asci, F., D'Onofrio, V., Sveva, V., Bologna, M., Fabbrini, G., Berardelli, A. and Suppa, A. (2020). "Enhancing Gamma Oscillations Restores Primary Motor Cortex Plasticity in Parkinson's Disease." J Neurosci **40**(24): 4788-4796.PMC7294804

Headley, D. B. and Weinberger, N. M. (2011). "Gamma-band activation predicts both associative memory and cortical plasticity." J Neurosci **31**(36): 12748-12758.PMC3180928

Hochberg, L. R., Bacher, D., Jarosiewicz, B., Masse, N. Y., Simeral, J. D., Vogel, J., Haddadin, S., Liu, J., Cash, S. S., van der Smagt, P. and Donoghue, J. P. (2012). "Reach and grasp by people with tetraplegia using a neurally controlled robotic arm." Nature **485**(7398): 372-375

Hortal, E., Planelles, D., Resquin, F., Climent, J. M., Azorin, J. M. and Pons, J. L. (2015). "Using a brain-machine interface to control a hybrid upper limb exoskeleton during rehabilitation of patients with neurological conditions." J Neuroeng Rehabil **12**: 92.PMC4609472

King, C. E., Dave, K. R., Wang, P. T., Mizuta, M., Reinkensmeyer, D. J., Do, A. H., Moromugi, S. and Nenadic, Z. (2014). "Performance assessment of a brain-computer interface driven hand orthosis." Ann Biomed Eng **42**(10): 2095-2105

Korenberg, M. J. and Hunter, I. W. (1986). "The identification of nonlinear biological systems: LNL cascade models." Biol Cybern **55**(2-3): 125-134

Krucoff, M. O., Rahimpour, S., Slutzky, M. W., Edgerton, V. R. and Turner, D. A. (2016). "Enhancing Nervous System Recovery through Neurobiologics, Neural Interface Training, and Neurorehabilitation." Front Neurosci **10**: 584.PMC5186786

Larzabal, C., Bonnet, S., Costecalde, T., Auboiroux, V., Charvet, G., Chabardes, S., Aksenova, T. and Sauter-Starace, F. (2021). "Long-term stability of the chronic epidural wireless recorder WIMAGINE in tetraplegic patients." J Neural Eng **18**(5)

Leinders, S., Vansteensel, M. J., Branco, M. P., Freudenburg, Z. V., Pels, E. G. M., Van der Vijgh, B., Van Zandvoort, M. J. E., Ramsey, N. F. and Aarnoutse, E. J. (2020). "Dorsolateral prefrontal cortex-based control with an implanted brain-computer interface." Sci Rep **10**(1): 15448.PMC7508852

Li, Y., Wang, P. T., Vaidya, M. P., Flint, R. D., Liu, C. Y., Slutzky, M. W. and Do, A. H. (2020a). "Electromyogram (EMG) Removal by Adding Sources of EMG (ERASE)-A Novel ICA-Based Algorithm for Removing Myoelectric Artifacts From EEG." Front Neurosci **14**: 597941.PMC7873899

Li, Y., Wang, P. T., Vaidya, M. P., Flint, R. D., Liu, C. Y., Slutzky, M. W. and Do, A. H. (2020b). "Refinement of High-Gamma EEG Features From TBI Patients With Hemicraniectomy Using an ICA Informed by Simulated Myoelectric Artifacts." Front Neurosci **14**: 599010.PMC7732541

Makeig, S. (1993). "Auditory event-related dynamics of the EEG spectrum and effects of exposure to tones." Electroencephalogr Clin Neurophysiol **86**(4): 283-293

Mansour, S., Ang, K. K., Nair, K. P. S., Phua, K. S. and Arvaneh, M. (2022). "Efficacy of Brain-Computer Interface and the Impact of Its Design Characteristics on Poststroke Upper-limb Rehabilitation: A Systematic Review and Meta-analysis of Randomized Controlled Trials." Clin EEG Neurosci **53**(1): 79-90.PMC8619716

Moses, D. A., Metzger, S. L., Liu, J. R., Anumanchipalli, G. K., Makin, J. G., Sun, P. F., Chartier, J., Dougherty, M. E., Liu, P. M., Abrams, G. M., Tu-Chan, A., Ganguly, K. and Chang, E. F. (2021). "Neuroprosthesis for Decoding Speech in a Paralyzed Person with Anarthria." N Engl J Med **385**(3): 217-227

Mrachacz-Kersting, N., Jiang, N., Stevenson, A. J., Niazi, I. K., Kostic, V., Pavlovic, A., Radovanovic, S., Djuric-Jovicic, M., Agosta, F., Dremstrup, K. and Farina, D. (2016). "Efficient neuroplasticity induction in chronic stroke patients by an associative brain-computer interface." J Neurophysiol **115**(3): 1410-1421.PMC4808132

No, M. M. (1976). Aids to the examination of the peripheral nervous system, HMSO, London.

Nowak, M., Hinson, E., van Ede, F., Pogosyan, A., Guerra, A., Quinn, A., Brown, P. and Stagg, C. J. (2017). "Driving Human Motor Cortical Oscillations Leads to Behaviorally Relevant Changes in Local GABAA Inhibition: A tACS-TMS Study." J Neurosci **37**(17): 4481-4492.PMC5413186

Oostenveld, R. and Praamstra, P. (2001). "The five percent electrode system for high-resolution EEG and ERP measurements." Clin Neurophysiol **112**(4): 713-719

Pels, E. G. M., Aarnoutse, E. J., Leinders, S., Freudenburg, Z. V., Branco, M. P., van der Vijgh, B. H., Snijders, T. J., Denison, T., Vansteensel, M. J. and Ramsey, N. F. (2019). "Stability of a chronic implanted brain-computer interface in late-stage amyotrophic lateral sclerosis." Clin Neurophysiol **130**(10): 1798-1803.PMC6880281

Pistohl, T., Schulze-Bonhage, A., Aertsen, A., Mehring, C. and Ball, T. (2012). "Decoding natural grasp types from human ECoG." Neuroimage **59**(1): 248-260

Ramos-Murguialday, A., Broetz, D., Rea, M., Laer, L., Yilmaz, O., Brasil, F. L., Liberati, G., Curado, M. R., Garcia-Cossio, E., Vyziotis, A., Cho, W., Agostini, M., Soares, E., Soekadar, S., Caria, A., Cohen, L. G. and Birbaumer, N. (2013). "Brain-machine interface in chronic stroke rehabilitation: a controlled study." Ann Neurol **74**(1): 100-108.PMC3700597

Rastogi, A., Vargas-Irwin, C. E., Willett, F. R., Abreu, J., Crowder, D. C., Murphy, B. A., Memberg, W. D., Miller, J. P., Sweet, J. A., Walter, B. L., Cash, S. S., Rezaii, P. G., Franco, B., Saab, J., Stavisky, S. D., Shenoy, K. V., Henderson, J. M., Hochberg, L. R., Kirsch, R. F. and Ajiboye, A. B. (2020). "Neural Representation of Observed, Imagined, and Attempted Grasping Force in Motor Cortex of Individuals with Chronic Tetraplegia." Sci Rep **10**(1): 1429.PMC6989675

Schneider, A. L. C., Wang, D., Gottesman, R. F. and Selvin, E. (2021). "Prevalence of Disability Associated With Head Injury With Loss of Consciousness in Adults in the United States: A Population-Based Study." Neurology **97**(2): e124-e135.PMC8279570

Silversmith, D. B., Abiri, R., Hardy, N. F., Natraj, N., Tu-Chan, A., Chang, E. F. and Ganguly, K. (2021). "Plug-and-play control of a brain-computer interface through neural map stabilization." Nat Biotechnol **39**(3): 326-335

Slutzky, M. W. (2019). "Brain-Machine Interfaces: Powerful Tools for Clinical Treatment and Neuroscientific Investigations." Neuroscientist **25**(2): 139-154.PMC6611552

Slutzky, M. W. and Flint, R. D., 3rd (2017). "Physiological Properties of Brain Machine Interface Input Signals." J Neurophysiol: jn 00070 02017

Soekadar, S. R., Birbaumer, N., Slutzky, M. W. and Cohen, L. G. (2015). "Brain-machine interfaces in neurorehabilitation of stroke." Neurobiol Dis **83**: 172-179

Stark, E. and Abeles, M. (2007). "Predicting movement from multiunit activity." J Neurosci **27**(31): 8387-8394

Traub, R. D., Spruston, N., Soltesz, I., Konnerth, A., Whittington, M. A. and Jefferys, G. R. (1998). "Gamma-frequency oscillations: a neuronal population phenomenon, regulated by synaptic and intrinsic cellular processes, and inducing synaptic plasticity." Prog Neurobiol **55**(6): 563-575

Vaidya, M., Flint, R. D., Wang, P. T., Barry, A., Li, Y., Ghassemi, M., Tomic, G., Yao, J., Carmona, C., Mugler, E. M., Gallick, S., Driver, S., Brkic, N., Ripley, D., Liu, C., Kamper, D., Do, A. H. and Slutzky, M. W. (2019). "Hemicraniectomy in traumatic brain injury: a noninvasive platform to investigate high gamma activity for brain machine interfaces." IEEE Trans Neural Syst Rehabil Eng

Vidoni, E. D., Acerra, N. E., Dao, E., Meehan, S. K. and Boyd, L. A. (2010). "Role of the primary somatosensory cortex in motor learning: An rTMS study." Neurobiol Learn Mem **93**(4): 532-539

Virani, S. S., Alonso, A., Aparicio, H. J., Benjamin, E. J., Bittencourt, M. S., Callaway, C. W., Carson, A. P., Chamberlain, A. M., Cheng, S., Delling, F. N., Elkind, M. S. V., Evenson, K. R., Ferguson, J. F., Gupta, D. K., Khan, S. S., Kissela, B. M., Knutson, K. L., Lee, C. D., Lewis, T. T., Liu, J., Loop, M. S., Lutsey, P. L., Ma, J., Mackey, J., Martin, S. S., Matchar, D. B., Mussolino, M. E., Navaneethan, S. D., Perak, A. M., Roth, G. A., Samad, Z., Satou, G. M., Schroeder, E. B., Shah, S. H., Shay, C. M., Stokes, A., VanWagner, L. B., Wang, N. Y., Tsao, C. W., American Heart Association Council on, E., Prevention Statistics, C. and Stroke Statistics, S. (2021). "Heart Disease and Stroke Statistics-2021 Update: A Report From the American Heart Association." Circulation **143**(8): e254-e743

Voytek, B., Secundo, L., Bidet-Caulet, A., Scabini, D., Stiver, S. I., Gean, A. D., Manley, G. T. and Knight, R. T. (2010). "Hemicraniectomy: a new model for human electrophysiology with high spatio-temporal resolution." J Cogn Neurosci **22**(11): 2491-2502.2888789

Wang, P. T., King, C. E., McCrimmon, C. M., Lin, J. J., Sazgar, M., Hsu, F. P., Shaw, S. J., Millet, D. E., Chui, L. A., Liu, C. Y., Do, A. H. and Nenadic, Z. (2016). "Comparison of decoding resolution of standard and high-density electrocorticogram electrodes." J Neural Eng **13**(2): 026016

Zhuang, J., Truccolo, W., Vargas-Irwin, C. and Donoghue, J. P. (2010). "Decoding 3-D reach and grasp kinematics from high-frequency local field potentials in primate primary motor cortex." IEEE Trans Biomed Eng **57**(7): 1774-1784.3049269